Original article

Hydrophobic performance of electrospun fibers functionalized with TiO$_2$ nanoparticles

Vânia Pais[1,2] **, Miguel Navarro**[1,2]**, Catarina Guise**[3]**,
Rui Martins**[3] **and Raul Fangueiro**[1,2,4]

Abstract

The development of materials with hydrophobic properties has been widely explored in areas such as textiles, health-care, sports, and personal protective equipment. Hydrophobic properties that arise from nanoparticles (nPs) directly promote other valuable properties, including self-cleaning capabilities, decreased bacterial growth, and increased comfort. In this study, biodegradable poly(ε-caprolactone) (PCL) nanofibers were functionalized by the incorporation of titanium dioxide (TiO$_2$) nPs to develop water-repellent materials. The membranes were produced through electrospinning, and variables such as the polymer concentration, nP concentration, and needle diameter were optimized to achieve PCL/TiO$_2$ composite fibers with water-repellent capabilities. The nanofibers were characterized by Fourier transform infrared spectroscopy, differential scanning calorimetry, thermogravimetric analysis, atomic force microscopy, scanning electron microscopy, transmission electron microscopy, and the water contact angle (WCA). In general, it was observed that the nanofibers presented higher roughness values when TiO$_2$ nPs were present and that this result promoted higher WCA values. The highest WCA value (156°) was obtained for the nanofiber mat produced with 20% weight-to-volume (w/v) PCL and 0.6% (w/v) TiO$_2$.

Wettability behavior plays a key role in a material's purposes and applications. This property is frequently determined by the contact angle (CA)—specifically the water contact angle (WCA)—measurement of a liquid droplet sitting on the surface of a material in a study. According to the values of the WCA, we can refer to a material as hydrophilic if it is between 0° and 90° or hydrophobic if it is between 90° and 180°. Inspired by nature, notable efforts have been made to establish materials capable of mimicking superhydrophobic behavior, as observed on a lotus leaf or rose petal.[1] Superhydrophobic materials repel water droplets by rolling them off and have WCA values higher than 150°.[2–4]

Eventually, particles caught by water droplets, such as dust or pollution, are also washed off surfaces in self-cleaning behaviors.[1] According to several authors, this interaction of liquids with surfaces can be described as a function of physical and chemical aspects, namely microtopography and surface chemistry.[5,6] A model to clarify this relationship in rough surfaces was developed by Robert N Wenzel in 1936.[7] Later, the efforts of Cassie and Baxter[8] resulted in a mathematical model for this behavior that could be applied to heterogeneous material surfaces, such as textiles or non-woven fabrics.

The development of materials and technologies with this superhydrophobic ability has been widely explored

[1]Fibrenamics, University of Minho, Portugal
[2]Centre for Textile Science and Technology (2C2T), University of Minho, Portugal
[3]Inovafil Fiação S.A, Portugal
[4]Department of Mechanical Engineering, University of Minho, Portugal

Corresponding author:
Vânia Nascimento Pais, UMinho Campus de Azurém, Av. da Universidade, 4 Guimarães, 4800-058 Portugal.
Email: vaniapais@fibrenamics.com

given the high potential value for a wide variety of products, such as anti-biofouling paints for boats, anti-stick coatings to repel snow on antennas and windows, self-cleaning windshields for automobiles, stain-resistant textiles, anti-soiling coatings, and oil/water separation.[4] In particular, self-cleaning is one of the most convenient features of superhydrophobic surfaces, so it is a current hot topic in areas such as product development.[9,10] In this particular case, when the contamination is sufficiently thick and the particle size of contaminants exceeds the pore size of the surface, the superhydrophobicity of the surface will be able to remove those contaminants by rinsing with water drops.[9] However, there are only a limited number of studies that look in detail at how this property works.

In recent years, various techniques have been studied to produce surfaces that mimic this natural super-hydrophobic effect. Notable among these are technological processes like the layer-by-layer approach to increasing surface roughness and electrospinning.[4] Electrospinning plays a major role in all such approaches due to its simplicity and versatility, which allows the production of membranes composed of fibers with different diameters, distinct compositions, and additives. This technology also allows for the manipulation of the properties, such as roughness, of the membranes that are produced. In addition to the purposes referred to, electrospinning is a promising and highly applicable technology in other fields, ranging from drug delivery[11] to air filtration,[12] and even to sensitive detection techniques,[13] as seen in the exponential growth in the number of scientific publications related to the electrospinning technique.[14]

Poly(e-caprolactone) (PCL) is a polymer composed of hydrophilic (-COOH, -OH) and hydrophobic (-$[CH_2]_5$) molecular groups. PCL is frequently used in the polymeric solution due to its biocompatibility, slow biodegradation, and good mechanical properties when produced by the electrospinning technique, which result in advanced materials capable of performing in a broad spectrum of applications.[14] According to Wang et al.,[5] when a thin film of PCL is under its phase transition temperature with a WCA of around 87° at 25°C, it will behave in a hydrophobic manner due to hydrophobic groups on its surface. However, once the temperature is increased to 60°C, PCL can undergo molecular reorientation, and even the presence of water can stimulate this reorientation, resulting in hydrophilic groups that face the surface, which decreases the WCA to the value of 59°.

In the present work, we aim to determine the wettability for electrospun nanofibers produced from a PCL polymer combined with titanium oxide (TiO_2) nanoparticles (nPs) to develop superhydrophobic structures. The use of TiO_2 in textiles has been a focus for

numerous research groups over the last decade, namely for ultraviolet (UV) protective, antibacterial, or even self-cleaning purposes.[15] TiO_2 nPs have three most common structures—the anatase, rutile, or brookite forms.[15] In the case of anatase TiO_2, thin films behave in a hydrophobic manner, although their wettability can be modulated as described by Zheng et al.[16] In addition to this property, Bajsić et al.[17] describe the biocompatibility and thermal stability after UV irradiation of PCL electrospun nanofibers functionalized with TiO_2 nPs, thus demonstrating the characteristic photocatalytic activity of TiO_2 and its influence on PCL degradation under UV light.

However, despite many studies showing the effectiveness of the combination of electrospinning-produced PCL nanofibers and TiO_2 nPs for tracing pollutants, photocatalysis, and antibacterial ability,[18] wettability behavior is still largely overlooked in the literature. Most of the studies developed in this domain make use of coatings to grant superhydrophobic behavior to the material's surface. There are a few works being developed that apply the electrospinning technique—for example, those developed by Yin et al.[18] In this study, the authors developed membranes that repel water and oil. To produce the polymer matrix, the electrospinning technique was applied, and then the surface was coated with nPs with a spraying method. The results of this study are very promising; however, they still require a two-step production process to obtain water-repellent samples. In the present work, we describe and discuss a novel and innovative approach that takes advantage of the synergistic effect of combining TiO_2 nPs and electrospinning technology to produce superhydrophobic mats of nanofibers in one single step.

Materials and methods

Materials

PCL pellets ($[C_6H_{10}O_2]_n$, average M_w 80.000 g/mol) obtained from Sigma-Aldrich were used as a polymer matrix. Titanium dioxide nPs in anatase conformation (TiO_2, average particle size 10–30 nm, 99.5% purity) were supplied by SkySpring Nanomaterials, Inc. (Houston, TX 77082, USA). The solvents chloroform and N,N-dimethylformamide (DMF) were obtained from Fisher Scientific (USA).

Preparation of PCL and PCL/TiO$_2$ fibers by electrospinning

The polymer solution concentration ranged from 15% to 20% (w/v) in chloroform:DMF (8:2 v/v) and was prepared by the dissolution of PCL in chloroform for

3 hours at 30°C with constant stirring. At this point, the dynamic viscosity of the solutions was measured with a Myr Rotary Viscometer Serie VR 3000 (VISCOTECH HISPANIA S.L.).

DMF was added due to its polyelectrolytic behavior, which allows for better electrical conductivity, dielectric constant, surface tension, and viscosity. The boiling point of DMF (153°C) is higher than that of chloroform (61.6°C), which decreases the rate of evaporation while producing nanofibers with electrospinning, allowing us to increase the distance between the collector and the needle. These factors promote better results in fiber morphology and decrease fiber diameter.[19] For the TiO_2 nP content, assays were performed using concentrations of 0.5%, 0.6%, and 0.7% (w/v). After being completely resuspended in DMF and subjected to sonication for 1 hour at 39 kHz, the nP solution was added to the polymer solution under constant stirring until complete homogenization occurred at $60\% \pm 5$ RH (relative humidity) and $20°C \pm 2$.

PCL and PCL/TiO_2 webs were produced by fiber deposition using the electrospinning technique. This process was performed using MECC Co., Ltd (NF-103, origin Japan) equipment. The polymeric solution was loaded into a syringe with a metal needle, and the fibers were collected in a metallic planar collector whose dimensions were 25 cm length by 15 cm width. Different needle diameters were tested: 0.25, 0.33, 0.41, and 0.61 mm. Regarding experimental conditions, all electrospinning procedures were performed using an applied voltage of 25 kV, a feed rate equal to 2 mL/h, and a tip-to-collector distance of 24 cm. The electrospinning process was realized at $60\% \pm 5$ RH and $20°C \pm 2$. These fixed parameters were defined by previous studies developed by the group with a focus on the production of fibers with an optimized morphology and low fiber diameter.[20,21]

In this study, the three aforementioned parameters (polymer concentration, nP concentration, and needle diameter) were tested to achieve our purpose of identifying the optimal conditions for producing electrospun fiber webs with superhydrophobic properties. These three parameters significantly influence fiber morphology. In turn, fiber morphology affects hydrophobic behavior. To achieve this study's purpose, a set of electrospun fibers was produced within the fixed parameters defined in the electrospinning operation and the study conditions that are represented in Table 1 (polymer and nP concentration refer to the polymeric solution loaded onto the electrospinning equipment). With the combination of the variables, a total of 24 fiber webs was obtained and further characterized in terms of properties and functionality.

Table 1. Parameters tested during the production of electrospun fibers with water-repellent abilities

[PCL] (%) (w/v)	[TiO₂] (%) (w/v)	Needle diameters (mm)
15	0.5	0.61
20	0.6	0.41
	0.7	0.33
		0.25

PCL: poly(ε-caprolactone).

Characterization techniques

The morphology of the electrospun fibers was assessed using field emission scanning electron microscopy (FESEM). The analyses were performed using a NOVA 200 Nano scanning electron microscope from the FEI Company (Hillsboro, OR, USA). To achieve an increased image quality considering the nature of the materials, all samples were vacuum metalized with a thin film of gold-palladium (Au-Pd) before the analysis. The average values of the fiber diameters were calculated by taking measurements from different regions using ImageJ software.[22] The presence and distribution of TiO_2 nPs were confirmed by transmission electron microscopy (TEM) using a JEOL JEM 2100 80–200 kV. The roughness of the produced fibers was evaluated by atomic force microscopy (AFM) using a NanoScopell operating in tapping mode. The AFM images were taken over scanning areas of $20 \times 20\,\mu m^2$ followed by $1 \times 1\,\mu m^2$.

The chemical composition and the structural aspects of the PCL and PCL/TiO_2 electrospun fibers were analyzed using Fourier transform infrared spectroscopy (FTIR) coupled with the attenuated reflection (ATR) technique using IRAffinity-1S, SHIMADZU equipment (Kyoto, Japan). All spectra were obtained in the transmittance mode and resulted from the accumulation of 45 scans within the wavelengths of 400–4000 cm^{-1}.

The thermal behavior of the electrospun fibers was assessed with a differential scanning calorimetry (DSC) analysis using equipment from Mettler Toledo under a nitrogen atmosphere while the samples (about 8–10 mg in weight) were heated from 0°C to 500°C with a heating rate of 10°C/min. Finally, a thermogravimetric analysis (TGA) of the electrospun fibers was performed with an STA 700 from HITACHI, and the samples were tested in the temperature range from 25°C to 500°C at 5°C/min heating rates.

Wettability

Wettability in terms of water repellence was evaluated by measuring the WCA established between a drop of water and the samples produced through

electrospinning. This measurement was processed with a Contact Angle System OCA 15 goniometer coupled with a high-resolution digital camera. To perform the assay, a 5 µL drop of distilled water was dropped from a microsyringe onto the surface of the electrospun fiber webs. The measurements were taken in 10 different places, and the respective averages and mean deviations were calculated. The following determinations were made: when the WCA was less than 90°, the samples were considered hydrophilic; when the angle was between 90° and 150°, the samples were considered hydrophobic; and when the angle was above 150°, the samples were considered superhydrophobic.[3] To assess the significance of the differences in the results, a statistical analysis was performed using a one-way analysis of variance (ANOVA) for a significance level of $P = 0.05$.

Results and discussion

Electrospun fiber characterization

Results of Fourier transform infrared spectroscopy. The FTIR spectra of fibers produced with a needle diameter of 0.41 mm are shown in Figure 1. Due to the similarity between the samples with nPs, only the results related to 20% (w/v) PCL and 20% (w/v) PCL_0.6% (w/v) TiO₂ are represented. From the figure, we can identify two sharp bands located at 2866 and 2943 cm⁻¹, usually related to the alkyl C-H group of the PCL's hydrocarbon. As we moved to higher frequencies, a signal located at 1721 cm⁻¹ arose, typically attributed to the stretching vibration of the PCL's carbonyl groups (C=O). The peak at 1219 cm⁻¹ corresponded to the vibration of the C-C and C-O groups. As we reached

1161 cm⁻¹, a signal resulting from the deformation of -CH₂- groups of PCL appeared.[17,23]

A typical FTIR spectra of TiO₂ is characterized by a rapid decline in transmission around 800 cm⁻¹, which is the result of the Ti-O bond vibration.[24] In the Figure 1 FTIR spectra, TiO₂ vibration caused a broad band between 450 and 915 cm⁻¹. This result confirms the successful incorporation of TiO₂ nPs during the preparation of the polymer solution and the presence of TiO₂ nPs in the electrospun fibers.

Differential scanning calorimetry and thermogravimetric analysis. Figure 2 shows the DSC curves for electrospun PCL and PCL/TiO₂ fibers. The DSC curves of electrospun PCL and PCL/TiO₂ fibers revealed two distinct sets of signals. We can confirm that the temperatures of the phase changes were similar in both conditions, regardless of the presence or absence of nPs.

In Figure 2, we can identify a signal around 60°C that is caused by the melting point (T_m) of PCL. Therefore, the phase transition of the electrospun fibers studied was about 60°C and was under the T_m noted for the PCL polymer.[24,25] At approximately 350°C, another endothermic peak occurred. When comparing this point to the TGA curve represented in Figure 3, it is possible to directly relate the change of the physical state represented in the DSC curve to the single-step degradation of the electrospun fibers (visible in the TGA curve). Indeed, by observing the TGA plot, it is clear that the rapid decline in values started at 350°C.

Comparing both of these results, it is possible to conclude that this is the point where the electrospun fibers began to thermally decompose, resulting in an almost total loss of the sample mass (degradation). From the TGA curve, it is evident that the presence
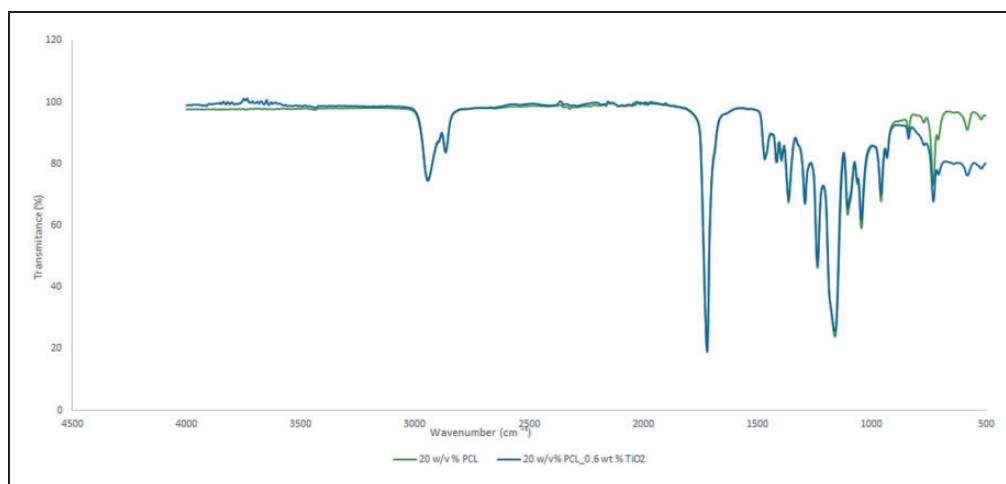

Figure 1. Fourier transform infrared spectra of electrospun poly(ε-caprolactone) (PCL) and PCL/TiO₂ fibers produced with a 0.41 mm needle diameter.
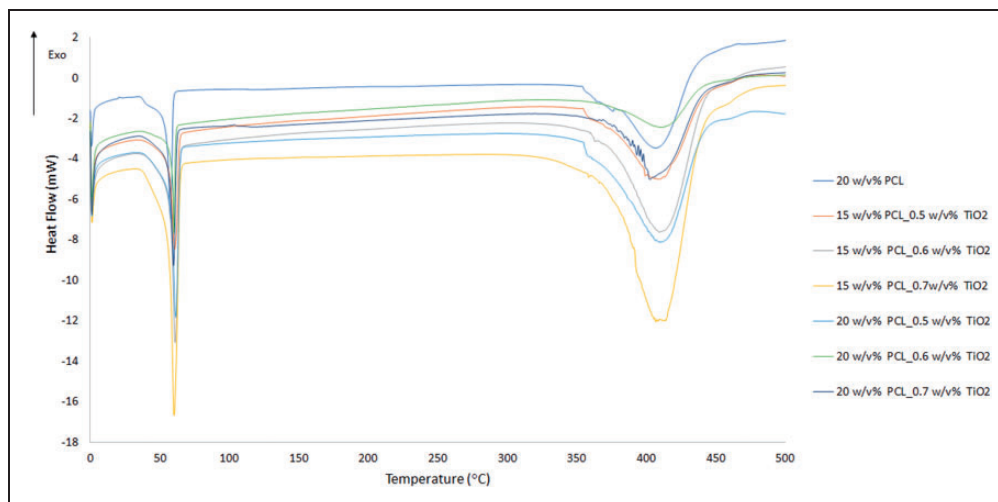
Figure 2. Differential scanning calorimetry curves of electrospun poly(ε-caprolactone) (PCL) and PCL/TiO$_2$ fibers produced with a 0.41 mm needle diameter.
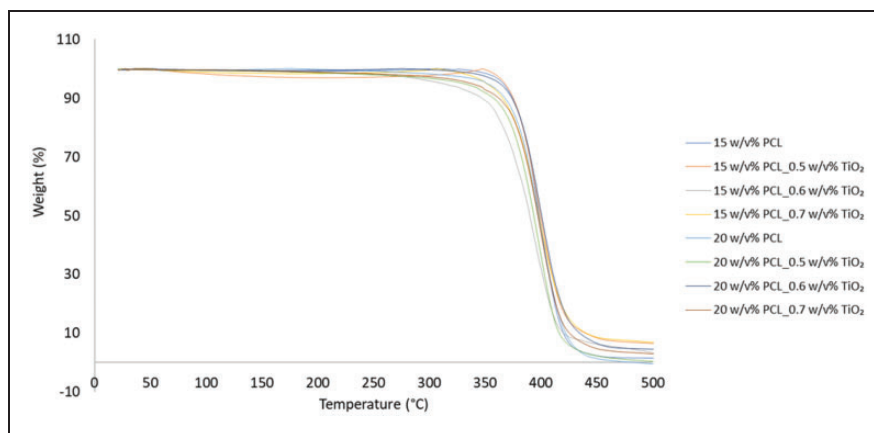

Figure 3. Thermogravimetric analysis curves of electrospun poly(ε-caprolactone) (PCL) and PCL/TiO$_2$ fibers produced with a 0.41 needle diameter.

of nPs did not change the thermal degradation mechanism of the PCL polymer. The only effect of the nPs was one we expected: a final residue after the performance of the TGA analysis. Also, the samples related to a PCL concentration of 15% w/v plus nPs had a higher amount of residual mass. This result makes sense in that a lower amount of PCL implies that the apparent same theoretical proportion of nPs is slightly higher because, after solvent evaporation, the fibers keep 100% PCL + TiO$_2$, which means that 0.6% w/v TiO$_2$ (for example) is different in a solution with 15% w/v PCL or 20% w/v PCL.

Morphological analysis

The morphological structure of the electrospun fibers was observed with scanning electron microscopy (SEM) images, which allowed an analysis of both nP distribution and the type of fibers produced. Figure 4 shows the SEM images of electrospun fibers produced with a 0.41 mm needle diameter and a polymer concentration of 20% (w/v) PCL plus the different concentrations of nPs tested (0%, 0.5%, 0.6%, and 0.7% weight–volume ratio).

The electrospun fibers showed a cylindrical shape with a few random beads formed, resulting from an irregular diameter increase at some points. The bead formation matches the main purpose of this work, as these formations are directly related to hydrophobic behavior, as reported by Huan et al.[26] in their work relating the presence of beads among nanowebs and hydrophobic behavior, which occurs due to a roughness increase. In addition, a noticeable increase in the number of beads was observed in the fibers with more nPs.
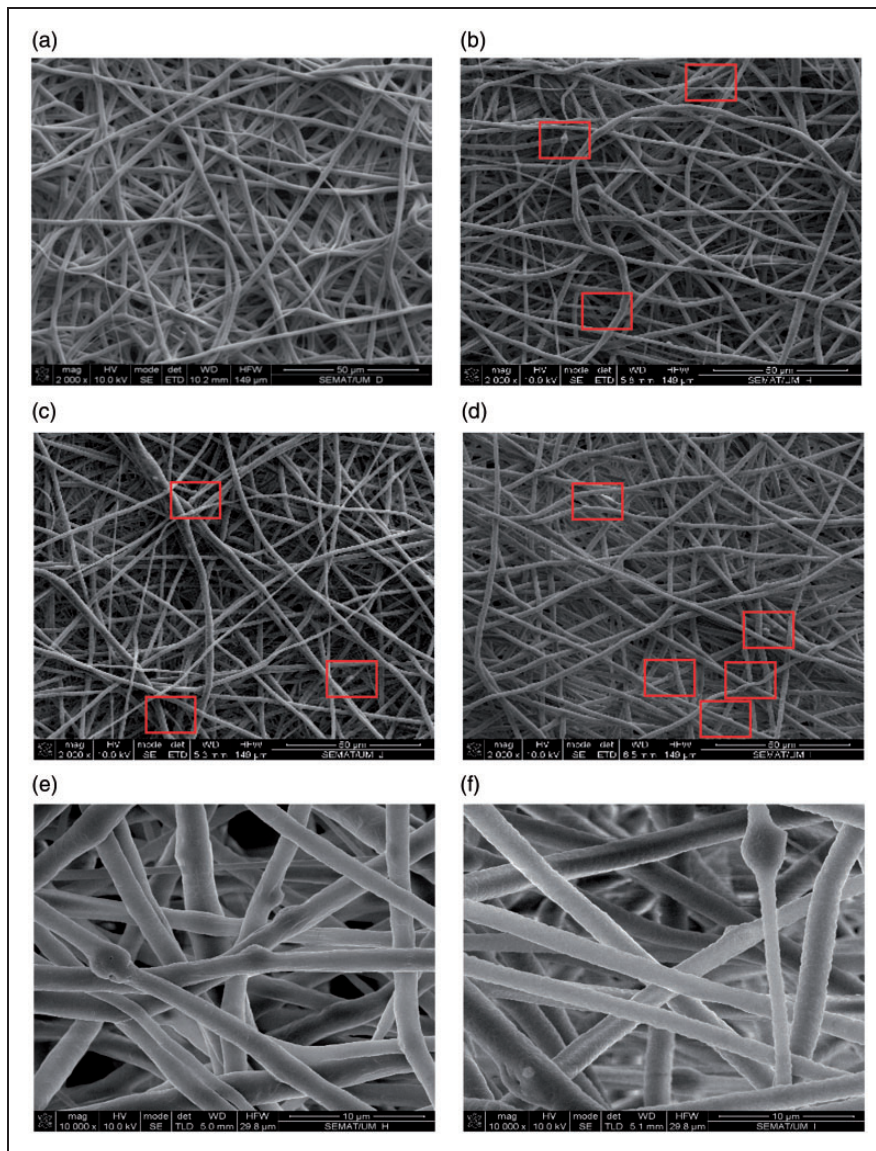
Figure 4. Scanning electron microscopy images of the electrospun fibers produced with a 0.41 mm needle diameter and 20% w/v poly(e-caprolactone) (PCL), 0% w/v TiO$_2$ (a), 0.5% w/v TiO$_2$ (b), 0.6% w/v TiO$_2$ (c), and 0.7% w/v TiO$_2$ (d); morphology of beaded fibers with a 0.41mm needle diameter and 20% w/v PCL, 0.6% w/v TiO$_2$ (e), and 0.7% w/v TiO$_2$ (f) (red boxes represent beads – color online only).

The successful incorporation of nPs in the fibers was also confirmed by TEM analysis. In the images we obtained, some black points were seen that correspond to the TiO$_2$ nPs. As shown in Figure 5, we were also able to confirm the uniform distribution of TiO$_2$ nPs in the fibers—with the formation of random agglomerations.

Finally, the different nP concentrations did not appear to negatively affect fiber morphology or the presence and distribution of nPs. The major difference observed in the morphology of the fiber mats with the addition of TiO$_2$ nPs was an increase in roughness. To confirm this statement, an AFM analysis was

performed, the results of which are represented in Table 2. Figure 6 shows a few of the images we obtained.

The AFM results indicate an increase in the roughness of the produced fibers as the concentration of nPs increased. When comparing the two samples with polymer concentrations equal to 15% and 20% w/v PCL without nPs, we concluded that the increase in polymer concentration also promoted higher roughness values. The perfect confluence of roughness, a porous structure, and bead formation promoted greater air trapping. An increase in bead formation was noted alongside an increased nP proportion, as represented
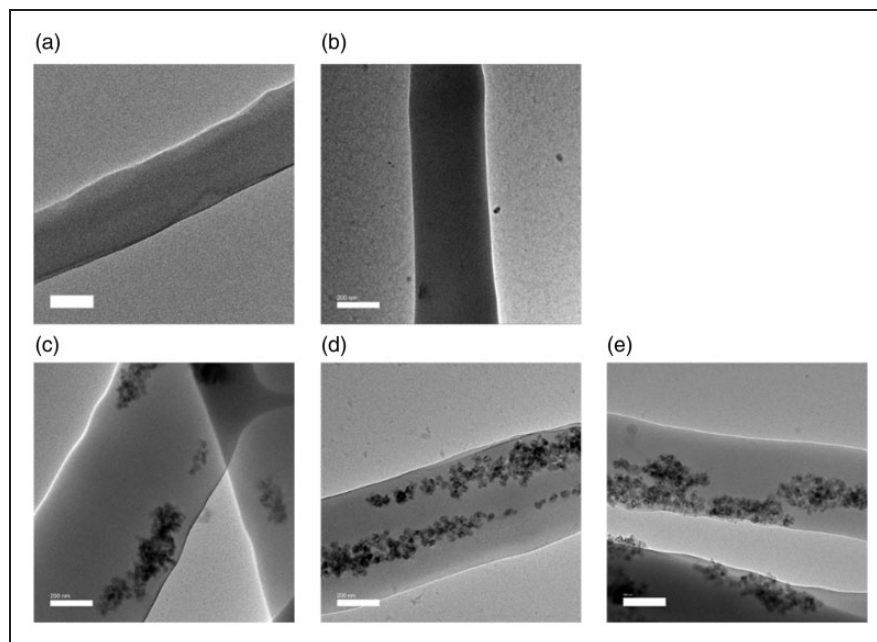
Figure 5. Transmission electron microscopy images of the electrospun fibers produced with 0.41 mm needle diameter with the corresponding proportion of 10% w/v poly(e-caprolactone) (PCL) (a), 20% w/v PCL (b), 20% w/v PCL _0.5% w/v TiO_2 (c), 20% w/v PCL _0.6% w/v TiO_2 (d), and 20% w/v PCL _0.7% w/v TiO_2 (e).

Table 2. The roughness of electrospun fibers produced with a 0.41 mm needle diameter containing different proportions of polymer and nanoparticles

	15% w/v PCL 0% w/v TiO_2	15% w/v PCL 0.5% w/v TiO_2	15% w/v PCL 0.6% w/v TiO_2	15% w/v PCL 0.7% w/v TiO_2	20% w/v PCL 0% w/v TiO_2
Average surface roughness (nm)	75.6	93.0	161.7	143.5	108.3

PCL: poly(ε-caprolactone).

in Figure 4. In line with the Cassie–Baxter model, the increase of beads and nP proportion benefits the hydrophobicity of the webs.[26] As referred to by Nuraje et al.,[27] this effect will impact the previously mentioned 'lotus effect,' with the right combination of surface chemistry and roughness resulting in super-hydrophobic behavior and promoting water droplet roll-off with cleaning effects.

The average diameter of the fibers produced with a needle diameter of 0.41 mm, 20% w/v PCL, and variable concentration of nPs is presented in Table 3. As the table shows, higher concentrations of PCL resulted in an increased spun fiber diameter because the diameters were measured on the nanoscale when we used the 15% w/v PCL solution, while the diameters were measured on the micro-scale for fibers with a 20% w/v PCL solution.

The viscosity of the solutions we used played a major role in the diameter of the fibers that were

produced, whereas larger concentrations of PCL were accompanied by an increase in viscosity values (see Table 3). Nezarati et al.[28] also noticed this relationship between viscosity and fiber diameter and attributed it to the electrospinning process. It was observed that electrospinning solutions with lower viscosity have an increased bead number due to the reduced viscoelastic capacity of the jet generated during the electrospinning process. In this study, we observed this effect in the different polymer proportions tested.

In the aforementioned study, Nezarati et al.[28] specified that bead formation occurs when the surface tension changes the jet to droplets. When the electrospinning process takes place, the electrostatic forces should overlap the surface tension to elongate and form the Taylor cone with subsequent solvent evaporation and fiber production. However, when the viscosity is not at ideal levels, this behavior between the electrostatic forces and surface tension may not
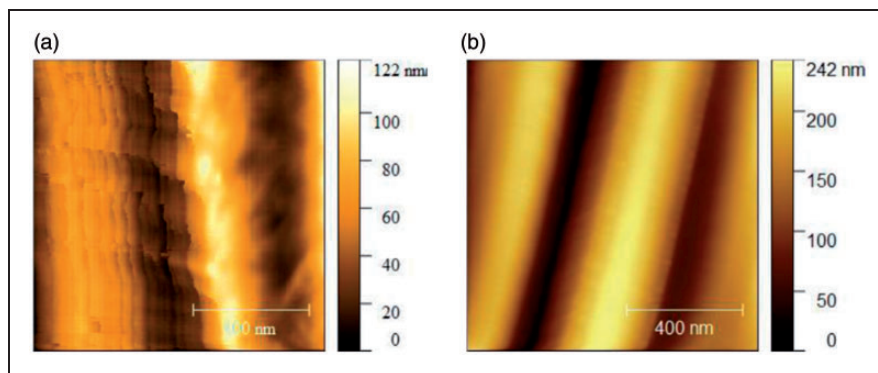
Figure 6. The surface roughness of the electrospun fibers of 15% w/v poly(e-caprolactone) (PCL) (a) and 15% w/v PCL_0.7% w/v PCL produced with a 0.41 needle diameter.

Table 3. The diameters of electrospun fibers produced with a 0.41 mm needle diameter containing different proportions of polymer and nanoparticles

Polymer concentration (%) (w/v)	15	20
Viscosity (mPa. s)	8900	12600
	Fiber diameters (nm)	
TiO_2 concentration (%) (w/v)		
0	1138 (717)	1864 (518)
0.5	553 (261)	1508 (547)
0.6	782 (267)	1575 (368)
0.7	839 (298)	1844 (567)

Note: standard deviations in parenthesis.

happen, thus affecting the formation of the beads. On the other hand, when the viscosity is too high, visco-elastic behavior amplifies the resistance to the axial stretching during whipping, resulting in fibers with larger diameters. Regarding the viscosity levels, we ensured that intermediate viscosity values were applied to avoid the problems presented by Nezarati et al.[28] These conclusions are in accordance with the research presented by Nezarati et al.,[28] where they observed that greater diameters were obtained when a higher polymer concentration/viscosity was applied. From the point of view of hydrophobicity, the relationship between higher PCL proportions and a greater fiber diameter is useful when considering the Cassie–Baxter effect—a liquid droplet on a rough surface with globules of air inside the surface turns to stay on the surface and does not penetrate the material.

Table 3 also presents the effect of the addition of nPs to the electrospun fibers. For both PCL concentrations tested, lower diameters were achieved when TiO_2 nPs were present. Several studies, such as Bortolassi et al.[29] and Demirsoy et al.,[30] describe the effects of nPs in electrospun fibers in terms of two major factors: (1)

the nPs can increase fiber diameter due to the addition of new material to the polymer matrix and/or because of the agglomeration of nPs in the fibers; and (2) nPs can decrease fiber diameter due to the increase of conductivity of the jet during electrospinning, causing the formation of thinner fibers.

These effects easily corroborate the formation of nanofibers instead of microfibers after the addition of TiO_2 nPs. This fact was confirmed by the metallic behavior of TiO_2 nPs, which increased in conductivity and caused the intensification of the charge density on the surface of the ejected solution during the electrospinning process. Polu and Rhee[31] also noticed an increase in conductivity with the addition of TiO_2 nPs, having reached an ionic conductivity value of $2.11 \times 10^{-5}\,S\,cm^{-1}$ at ambient temperature with the incorporation of 8 wt % of TiO_2. Lastly, from the observations shown in Table 3, we can confirm that with an increased nP concentration, a higher fiber diameter occurred as a result of the effect of this new material. The formation of agglomerations onto the fibers was also observed.

Chemical composition can also affect the hydrophobicity of the sample, depending on factors like the types and proportions of specific functional groups. From a morphological viewpoint, the consolidation of the three variables analyzed in this study will potentially affect hydrophobic intensity insofar as they influence aspects such as the number of fibers, the presence of irregular diameters, and density.

Hydrophobicity properties

In a further analysis, the wettability of the electrospun fibers was measured to determine the water repellency of the produced samples and the influence of TiO_2 and PCL concentrations on hydrophobic behavior. Figure 7 shows the mean value of the WCA obtained for the produced electrospun fibers. In Figure 8, the
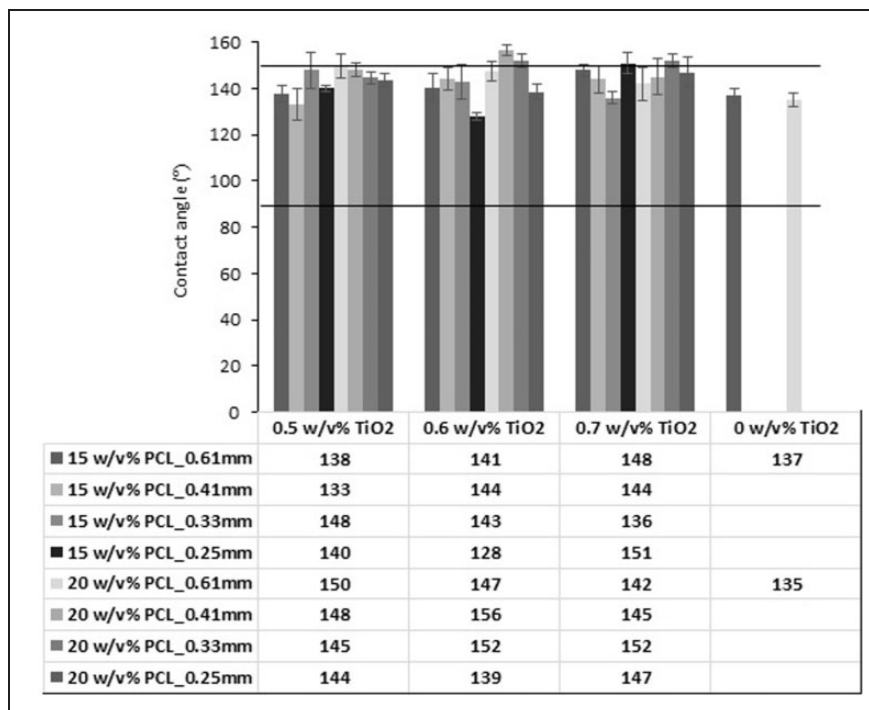
Figure 7. Water contact angles of fiber webs produced by electrospinning; horizontal black lines represent the minimum to achieve hydrophobicity (90°) and the minimum to be classified as superhydrophobic (150°). PCL: poly(ε-caprolactone).
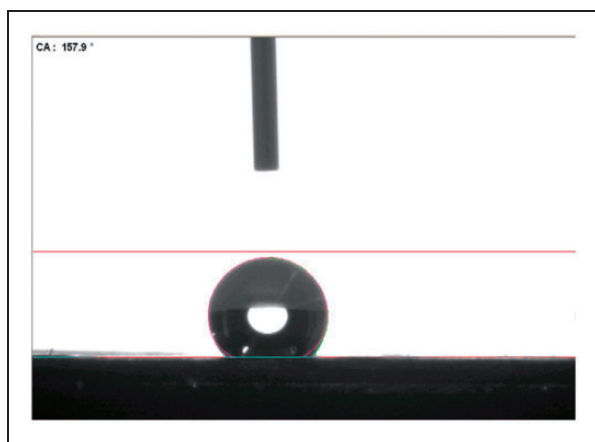
	0.5 w/v% TiO2	0.6 w/v% TiO2	0.7 w/v% TiO2	0 w/v% TiO2
■ 15 w/v% PCL_0.61mm	138	141	148	137
■ 15 w/v% PCL_0.41mm	133	144	144	
■ 15 w/v% PCL_0.33mm	148	143	136	
■ 15 w/v% PCL_0.25mm	140	128	151	
■ 20 w/v% PCL_0.61mm	150	147	142	135
■ 20 w/v% PCL_0.41mm	148	156	145	
■ 20 w/v% PCL_0.33mm	145	152	152	
■ 20 w/v% PCL_0.25mm	144	139	147	

Figure 8. Water contact angle of the fiber webs produced with 20 w/v% poly(ε-caprolactone) and 0.6% w/v TiO$_2$ with needle diameter equal to 0.41 mm.

water sessile drop on the fiber surface in the sample that achieved the highest WCA value is represented.

In Figure 7, it is clear that the complete set of fiber webs studied had either a hydrophobic or super-hydrophobic nature. For the samples obtained with a needle diameter of 0.61 mm, the samples incorporated with TiO$_2$ nPs had WCA values higher than the samples with no TiO$_2$ nPs. Hydrophobic behavior was

expected due to the hydrophobic characteristics of the PCL polymer and TiO$_2$ nPs. This result follows the SEM and AFM analyses by which we concluded that the presence of TiO$_2$ nPs promoted an increase in roughness, thereby ensuring superhydrophobia in samples.

To justify this result, we should consider the lotus effect, which can be mimicked on surfaces produced by the electrospinning technique. In nature, the surface of the lotus leaf is typically composed of hills and valleys of 3–10 μm that are coupled with particles on the nanoscale. The disposal of the micrometer-sized hills and valleys ensures low area-to-water contact, and the nanosized particles can prevent water penetration between these structures.

For instance, this effect predicts water droplet formations above the surface and a low roll-off angle.[4] When controlling the polymer matrix and the introduction of nPs through electrospinning, it is possible to mimic the hydrophobic effect described, as we can see in Figure 4. Electrospinning can produce fibers with nano and micro diameters. These fibers combined with particles on the nanoscale (10–30 nm) constitute the perfect conditions to create surfaces containing superhydrophobic properties, like those of the lotus leaf.

Therefore, when we are combining two ideas, such as electrospinning (which includes polymers and nPs)

and the concept of hydrophobicity, roughness will have a large effect on the final result. A considerable number of related studies previously established a direct relationship between the increase of roughness and the hydrophobic properties of the materials. The electrospun fibers have some roughness in their intrinsic properties, which is a consequence of the small diameters of fibers and their organization with or relation to each other. These studies also proved that the addition of nPs is a main cause of increased roughness.

This relationship was also confirmed in the present study, where a clear increase in the roughness of fibers containing nPs was detected through AFM analysis. This morphological behavior has consequences for hydrophobic properties—namely for the WCA values obtained. When observing the resultant WCA values, generally when nPs are present, the WCA values rise. The fibers composed only of PCL polymer had WCA values that qualified as hydrophobic, while some electrospun fibers incorporated with TiO_2 nPs achieved WCA values that were associated with superhydrophobic behaviors. These results can be justified by the roughness achieved when producing fibers using the electrospinning technique. However, higher WCA values in the fibers with TiO_2 nPs result from the presence of these nPs, which increase hydrophobic behavior and fiber roughness.

The chemical composition of the present components must also be considered. PCL polymer is known as a hydrophobic material due to some of its molecular groups ([$-CH_2$]$_5$). Therefore, from a chemical point of view, the hydrophobic properties observed in the fibers with a total absence of nPs are justified. The electrospun fibers produced with 15% and 20% (w/v) PCL achieved similar WCA results: 137° and 135°, respectively. These results show that the two electrospun fibers produced without the addition of nPs had a similar hydrophobic nature with no significant differences between them. According to Zheng et al.,[16] TiO_2 nPs may promote better hydrophobic properties. Zheng et al.[16] argue that TiO_2 nPs have fully stoichiometric interactions, which means that each titanium atom surrounded by two oxygen atoms can establish a chemical bond with a water molecule, thereby reducing the water penetration within the matrix.

Of the 24 electrospun webs produced, a total of five samples achieved WCA values corresponding to the superhydrophobic categorization: one with 0.5% (w/v) TiO_2 nPs, two with 0.6% (w/v) TiO_2 nPs, and two with 0.7% (w/v) TiO_2 nPs. The two highest proportions of nPs produced a significant number of samples with superhydrophobic properties. In fact, in the sample containing 0.5% (w/v) TiO_2, the WCA value was 150°, which is the minimum value to be characterized as a superhydrophobic sample. In contrast, when we analyzed the samples with high contents of TiO_2 nPs, larger WCA values were obtained—the web with 20% (w/v) PCL_0.6% (w/v) TiO_2_0.41 mm had the highest WCA value: 156° (superhydrophobic). This result was a consequence of the addition of TiO_2 nPs, which conferred a higher roughness to the surface. The statistical difference between the samples with different nP proportions was confirmed by an ANOVA. For example, when the concentration of the polymer is fixed at 20% (w/v) PCL and the needle diameter at 0.41 mm, the influence of the different nP proportions on the WCA can be studied. With these conditions, the P-value obtained was 0.013. Since this value is lower than 0.05, from a statistical point of view, this result means that the different WCAs obtained (when varying the nP proportion) have relevance and should be considered. The same methodology was applied to the other parameters.

No direct relationship was noted between needle diameter and the topology of the fibers produced. Macossay et al.[32] applied different needle diameters during electrospinning and observed a lack of relationship between the needle diameter used and the resulting average fiber diameter. They also observed that, when a smaller needle diameter was applied, a greater standard deviation relative to the mean fiber diameter was obtained. With a higher range of fiber diameter, fewer empty spaces occurred.

In this case, the ideal conditions described in the Cassie–Baxter effect were not achieved. The Cassie–Baxter effect indicates that when a liquid droplet is applied on a rough surface with globules of air trapped inside the surface, the droplet tends to become suspended and does not penetrate the surface. This trait is a peculiarity of hydrophobic behavior.[3] Thus, it is logical that, when a lower needle diameter is applied, the increased heterogeneity in the fiber diameter leads to increased packing (few empty spaces on the surface), which results in lower WCA values. This conclusion is supported by our results insofar as WCA values corresponding to the lower diameter needle were among the lowest values obtained. The exception was when the highest content of TiO_2 nPs was applied, in which case we suggest that the effect of roughness caused by nPs overlapped with the effect of fibers with similar diameters. This final statement emphasizes the relation observed between the presence of TiO_2 nPs and higher roughness values, which in turn increases the hydrophobic behavior.

Conclusions

Electrospun fibers composed of PCL polymer and TiO_2 nPs with superhydrophobic properties were designed and produced using an electrospinning technique.

This study produced several superhydrophobic conditions, the highest WCA value of which was 156°.

These results produced some important general conclusions.

1. When TiO_2 nPs are present, a great number of nanofiber nets achieve a WCA categorized as superhydrophobic. This result is a direct consequence of the hydrophobic behavior of TiO_2 and the increase in roughness caused by nPs. It was also noted that an increase in the PCL proportion promotes higher WCA values.
2. The essential role roughness plays in the achievement of hydrophobic and superhydrophobic properties was confirmed. Concerning the roughness, the AFM results also confirmed that the addition of nPs increases the roughness of electrospun fibers, which enhances water repellency, with a potential positive consequent effect on self-cleaning ability.
3. Although TiO_2 nPs play an essential role in producing water repellency, PCL polymer also has the ability to repel water, as WCA values between 90° and 150° were obtained for the samples without nPs. This result is a consequence of the morphology of the fibers produced with an electrospinning technique.
4. Using needles with small diameters promoted the production of more varied fiber diameters, thereby decreasing the Cassie–Baxter effect and the hydrophobic properties. This result was less notable with an increase in the concentration of nPs.

The present study confirms the hydrophobic and superhydrophobic characteristics of the nanofiber webs that were produced. These results were theoretically related with the Cassie–Baxter model, which justifies hydrophobic properties with a specific combination of surface chemistry and roughness promoting the roll-off of droplets and consequently producing a self-cleaning effect. In future studies, we intend to perform assays that further prove and corroborate these observations.

ORCID iD

Vânia Pais https://orcid.org/0000-0003-2584-9900

References

1. Liu M, Zheng Y, Zhai J, et al. Bioinspired super-antiwetting interfaces with special liquid-solid adhesion. *Acc Chem Res* 2010; 43: 368–377.
2. Wang X, Ding B, Yu J, et al. Engineering biomimetic superhydrophobic surfaces of electrospun nanomaterials. *Nano Today* 2011; 6: 510–530.
3. Darmanin T and Guittard F. Recent advances in the potential applications of bioinspired superhydrophobic materials. *J Mater Chem A* 2014; 2: 16319–16359.
4. Asmatulu R, Ceylan M and Nuraje N. Study of superhydrophobic electrospun nanocomposite fibers for energy systems. *Langmuir Lett* 2011; 27: 504–507.
5. Wang C-F, Liao C-S, Kuo S-W, et al. Tunable wettability of carbon nanotube/poly (ε-caprolactone) hybrid films. *Appl Surf Sci* 2011; 257: 9152–9157.
6. Feng X, Feng L, Jin M, et al. Reversible superhydrophobicity to super-hydrophilicity transition of aligned ZnO nanorod films. *J Am Chem Soc* 2004; 126: 62–63.
7. Wenzel RN. Resistance of solid surfaces to wetting by water. *Ind Eng Chem* 1936; 28: 988–994.
8. Cassie ABD and Baxter S. Wettability of porous surfaces. *Trans Faraday Soc* 1944; 40: 546–551.
9. Geyer F, et al. When and how self-cleaning of superhydrophobic surfaces works. *Sci Adv* 2020; 6: eaaw9727.
10. Latthe SS, et al. Self–cleaning superhydrophobic coatings: potential industrial applications. *Prog Org Coatings* 2019; 128: 52–58.
11. Mickova A, et al. Core/shell nanofibers with embedded liposomes as a drug delivery system. *Biomacromolecules* 2012; 13: 952–962.
12. Liu C, et al. Transparent air filter for high-efficiency PM 2.5 capture. *Nat Commun* 2015; 6: 1–9.
13. Meng C, Xiao Y, Wang P, et al. Quantum-dot-doped polymer nanofibers for optical sensing. *Adv Mater* 2011; 23: 3770–3774.
14. Mochane MJ, Motsoeneng TS, Sadiku ER, et al. Morphology and properties of electrospun PCL and its composites for medical applications: a mini review. *Appl Sci (Switzerland)* 2019; 9: 1–17.
15. Radetić M. Functionalization of textile materials with TiO_2 nanoparticles. *J Photochem Photobiol C Photochem Rev* 2013; 16: 62–76.
16. Zheng JY, Bao SH, Guo Y, et al. Natural hydrophobicity and reversible wettability conversion of flat anatase TiO_2 thin film. *ACS Appl Mater Interfaces* 2014; 6: 1351–1355.
17. Bajsić EG, Mijović B, Penava NV, et al. The effect of UV irradiation on the electrospun PCL/TiO_2 composites fibers. *J Appl Polym Sci* 2016; 133: n/a-n/a.

18. Yin H, et al. Electrospun SiNPs/ZnNPs-SiO2/TiO2 nanofiber membrane with asymmetric wetting: ultra-efficient separation of oil-in-water and water-in-oil emulsions in multiple extreme environments. *Sep Purif Technol* 2020; 255: 1–11.

19. Hsu CM and Shivkumar S. N,N-dimethylformamide additions to the solution for the electrospinning of poly(ε-caprolactone) nanofibers. *Macromol Mater Eng* 2004; 289: 334–340.

20. Karagoz S, et al. Synthesis of Ag and TiO2 modified polycaprolactone electrospun nanofibers (PCL/TiO2-Ag NFs) as a multifunctional material for SERS, photocatalysis and antibacterial applications. *Ecotoxicol Environ Saf* 2019; 188: 1–10.

21. Francavilla P, Ferreira DP, Araújo JC, et al. Smart fibrous structures produced by electrospinning using the combined effect of PCL/graphene nanoplatelets. *Appl Sci* 2021; 11: 1–22.

22. Rueden CT, et al. ImageJ2: ImageJ for the next generation of scientific image data. *BMC Bioinformat* 2017; 18: 529.

23. Li R, Nie K, Shen X, et al. Biodegradable polyester hybrid nanocomposites containing titanium dioxide network and poly(ε-caprolactone): synthesis and characterization. *Mater Lett* 2007; 61: 1368–1371.

24. Saricam C, Okur N and Göcek İ. Functionalization of electrospun nanofibers by using titanium dioxide and 1,3,7-trimethyl xanthine for developing ultraviolet protection. *J Ind Text* 2019; 0: 1–17.

25. Borjigin M, Eskridge C, Niamat R, et al. Electrospun fiber membranes enable proliferation of genetically modified cells. *Int J Nanomed* 2013; 8: 855–864.

26. Huan S, et al. Effect of experimental parameters on morphological, mechanical and hydrophobic properties of electrospun polystyrene fibers. *Materials (Basel)* 2015; 8: 2718–2734.

27. Nuraje N, Khan WS, Lei Y, et al. Superhydrophobic electrospun nanofibers. *J Mater Chem A* 2012; 1: 1929–1946.

28. Nezarati RM, Eifert MB and Cosgriff-Hernandez E. Effects of humidity and solution viscosity on electrospun fiber morphology. *Tissue Eng C Meth* 2013; 19: 1–10.

29. Bortolassi ACC, et al. Efficient nanoparticles removal and bactericidal action of electrospun nanofibers membranes for air filtration. *Mater Sci Eng C* 2019; 102: 718–729.

30. Demirsoy N, et al. The effect of dispersion technique, silver particle loading, and reduction method on the properties of polyacrylonitrile–silver composite nanofiber. *J Ind Text* 2014; 0: 1–15.

31. Polu AR and Rhee HW. Effect of TiO2 nanoparticles on structural, thermal, mechanical and ionic conductivity studies of PEO12-LiTDI solid polymer electrolyte. *J Ind Eng Chem* 2016; 37: 347–353.

32. Macossay J, Marruffo A, Rincon R, et al. Effect of needle diameter on nanofiber diameter and thermal properties of electrospun poly(methyl methacrylate). *Polym Adv Technol* 2007; 18: 180–183.